Numerical algorithm for the determination of the potential of a conservative system from its normal mode spectra

Numerical algorithm for the determination of the potential of a conservative system from its normal mode spectra

C-P Sun†§, K Young† and J Zou‡

† Department of Physics, The Chinese University of Hong Kong, Hong Kong, People's Republic of China
‡ Department of Mathematics, The Chinese University of Hong Kong, Hong Kong, People's Republic of China
§ Institute of Theoretical Physics, Chinese Academy of Sciences, Beijing 100080, People's Republic of China

Abstract. An efficient numerical algorithm is developed for determining the potential of a conservative system described by a Klein–Gordon or Schrödinger equation from its normal mode spectra. The algorithm is based on first solving the linear problem of perturbative inversion by means of Tikhonov regularization, and then using a series of perturbative steps to approach the full potential by Newton's method. The algorithm is stable and convergence is rapid.

1. Introduction

In the general class of inversion problems, one tries to determine a system from its observables. The best known example is the attempt to determine a Hamiltonian operator (given its general form) from its eigenvalues—which is obviously much harder but at the same time much more useful than the corresponding forward problem of finding the eigenvalues from the Hamiltonian.

In this paper we consider the 1D Klein–Gordon (KG) equation

$$[\partial_t^2 - \partial_x^2 + V(x)]\Phi(x,t) = 0 \tag{1}$$

with a real potential $V(x)$, defined on a finite interval $I = [0, a]$, and suitable boundary conditions to be specified below. We seek an efficient and stable numerical algorithm for determining the potential $V(x)$ from the eigenfrequencies $\{\omega_n\}$, where each ω is defined in terms of the eigensolutions of (1), $\Phi(x,t) = f(x)e^{-i\omega t}$. We consider boundary conditions that define a conservative system (e.g., nodes or antinodes at the endpoints of the interval), so that ω is real. Inversion from the spectrum is important because frequencies can often be measured directly or extracted from the time-domain signal.

This eigenvalue problem is

$$[-\partial_x^2 + V(x)]f(x) = \lambda f(x) \tag{2}$$

where $\lambda = \omega^2$. This can also be regarded as the time-independent Schrödinger equation with $\lambda = \omega$. Historically, the interest was on the Schrödinger equation on a half-line $0 \leqslant x < \infty$, where x is in effect a radial variable, and in the determination of $V(x)$ from scattering data. Attempts to fit the nucleon–nucleon potential $V(x)$ from the measured phase shift $\delta(\lambda)$ led to ambiguous results, and thus prompted the question: can $V(x)$ be obtained uniquely from $\delta(\lambda)$?

The problem took a major turn when Bargmann [1] showed that inequivalent potentials can lead to the same phase shift. It soon became clear [2–7] that bound states must also be considered, and that $V(x)$ can be completely determined from three sets of information: (a) the phase shift $\delta(\lambda)$ for all $\lambda > 0$; (b) the bound state spectrum $\{\lambda_n\}$ (a finite number for short-ranged potentials of finite depth); and (c) a set of normalization constants $\{c_n\}$ for the bound states (e.g., the derivatives $f'(0)$ when the states are normalized to unity). The corollary that $[\delta(0) - \delta(\infty)]/\pi$ is related to the number of bound states is now widely known as Levinson's theorem. This development has been reviewed by many authors, e.g., Faddeev [8] and Dyson [9].

For a finite interval $I = [0, a]$, with nodal or antinodal boundary conditions at the endpoints, one would not refer to phase shifts. The inversion of such Sturm–Liouville systems from their spectral data alone was attacked by Borg [2], and pursued in detail by Levinson [3], Marchenko [4], Krein [5], Jost and Kohn [6] and Gelfand and Levitan [7]. It was shown that the data sets (b) and (c) (now referring to an infinite set of eigenstates) will be necessary and sufficient. Developments have been reviewed by Levitan [10].

It is also possible to require two other sets of data instead [2, 3, 11]: (b1) the eigenvalues $\{\lambda_n^{(1)}\}$ for $f(0) = f(a) = 0$ (the nodal problem); and (b2) the eigenvalues $\{\lambda_n^{(2)}\}$ for $f(0) = f'(a) = 0$ (the antinodal problem). The second set replaces the normalization conditions (c). It is heuristically reasonable that all information about the system can be obtained from its normal modes (NMs), because they are complete. The data (b1) alone are not enough, since the nodal problem cannot distinguish between $V(x)$ and $V(a - x)$; the data (b2) break the symmetry $x \mapsto a - x$.

These classical results on existence and uniqueness for the inversion problem are some 40–50 years old, but inversion algorithms [3, 11–13] proposed before recent advances in computational science are for the most part not practical. They involve, for example, the solution of a large number of coupled nonlinear ordinary differential equations [11, 12], or algebraic equations [13]. This paper develops a stable and efficient numerical algorithm using techniques that are now standard and well known.

Our strategy is based on first solving the easier problem of *perturbative inversion* (PI). Consider a known potential $V(x)$ with eigenvalues $\{\lambda_n\}$ subjected to an unknown perturbation $\Delta V(x)$, causing first-order shifts $\{\Delta \lambda_n\}$ in the eigenvalues. The problem is to obtain ΔV from $\{\Delta \lambda_n\}$. This is a linear problem, and a numerical scheme is developed, based on discretization of an integral equation. This scheme is presented in section 2 together with examples.

The more difficult problem is that of *total inversion* (TI), i.e., determining the potential V from the eigenvalues $\{\lambda_n\}$. An algorithm is developed, essentially Newton's method generalized to functionals, which makes use of PI to perform TI in an iterative manner. This formalism is presented in section 3, and examples are given to show that the convergence is rapid and the method is stable and accurate.

Concluding remarks are given in section 4, including a brief discussion on the possibility of generalizing to certain nonconservative systems—which are qualitatively different in that the eigenvalues are not real.

As a matter of notation, it will be convenient to extend the problem to the interval $[0, 2a]$, with all potentials symmetric about the mid-point $x = a$. Then the nodal problem on $[0, a]$ ($f(0) = f(a) = 0$) and the antinodal problem ($f(0) = f'(a) = 0$) translate respectively into the odd and even sectors on the extended interval, and both can be labelled together with one index $n = 1, 2, \ldots$†. Henceforth the perturbation will also be denoted as $v(x) \equiv \Delta V(x)$. The linear algebraic systems arising from the discretization of (2) and the Fredholm integral

---

† This notation only serves to simplify some formulae, but actual numerical computation is carried out on $[0, a]$ with the two spectra separately. One could also place the antinode at $x = 0$ rather than $x = a$ and extend to $[-a, a]$ instead.

equation below are solved using MATLAB.

2. Perturbative inversion

2.1. Integral equation

The forward perturbative problem gives

$$\Delta\lambda_n = \int_0^{2a} f_n^2(y)v(y)\,\mathrm{d}y \tag{3}$$

where the eigenfunctions f_n of the original unperturbed problem are assumed to be real and normalized on $[0, 2a]$. Multiplying by $f_n(x)^2/\sigma_n$ (where σ_n are positive numbers to be specified) and summing over n then leads to a Fredholm equation

$$\mu(x) = \int_0^a k(x, y)v(y)\,\mathrm{d}y \tag{4}$$

in which

$$\mu(x) = \sum_n \frac{\Delta\lambda_n}{\sigma_n} f_n^2(x) \tag{5}$$

is readily evaluated from the given spectral data and the known eigenfunctions of the unperturbed system. The real symmetric kernel is

$$k(x, y) = 2\sum_n \frac{f_n^2(x) f_n^2(y)}{\sigma_n}. \tag{6}$$

The PI problem is reduced to solving this integral equation to find $v(y)$. The classical existence and uniqueness theorems (applied to V and $V + \Delta V$) guarantee that there will be a unique solution for $v \equiv \Delta V$.

Formally, these sums do not converge in a pointwise sense without some regulators $\{\sigma_n\}$. Normalization implies that $f_n(x)^2 \sim \mathrm{O}(n^0)$ as $n \to \infty$. If the perturbation has a nonzero average, then we also have $\Delta\lambda_n \sim \mathrm{O}(n^0)$ as $n \to \infty$. One would need $\sigma_n \sim n^\rho$ with $\rho > 1$ to ensure pointwise convergence of the sums (5) and (6). On the other hand, if σ_n increases too rapidly with n, then one would lose information on the higher modes and hence the finer spatial structure.

Nevertheless, if these infinite sums are considered in the context of the integral equation (4), it is clear that only convergence in some weak sense is required, and depending on the test functions, possibly no regulators are needed. Indeed we have verified in some examples that $\sigma_n = 1$ still produces the correct answers. We shall not exploit this possibility, and have chosen $\sigma_n = n^2$ throughout, except where otherwise specified. In any event, the solution should be independent of the precise choice of $\{\sigma_n\}$, and this is verified numerically in some of the examples below.

2.2. Output least-squares method for ill-posed integral equations

While in principle a solution is guaranteed to exist, in practice the problem (4) is ill-posed because it may be unstable to noisy data: small changes in $\mu(x)$ could cause large changes in $v(x)$. To overcome this difficulty, we apply the output least-squares method combined with Tikhonov regularization [14] to map onto a nearby well-posed problem. The latter can then be solved numerically and stably. To do so, define an operator $K : L^2(0, a) \to L^2(0, a)$:

$$Kv(x) = \int_0^a k(x, y)v(y)\,\mathrm{d}y \tag{7}$$

for any $x \in [0, a]$. Then we formulate the integral problem as the following minimization problem over all $v \in L^2(0, a)$:

$$\min \|Kv - \mu\|^2 + \tilde{\alpha}\|v\|^2 \tag{8}$$

where $\tilde{\alpha} > 0$ is a regularization parameter, and $\|\cdot\|$ is the L^2 norm. This minimization problem has a unique solution, and the solution depends on $\tilde{\alpha}$ continuously [15].

We next discretize at N uniformly spaced points $x_n = nh, n = 0, \ldots, N$, with $h = a/N$. The trapezoidal rule leads to the following approximation:

$$Kv(x) = \sum_{n=1}^{N} \int_{x_{n-1}}^{x_n} k(x, y)v(y)\,\mathrm{d}y \approx \frac{h}{2}k(x, x_0)v_0 + h\sum_{n=1}^{N-1} k(x, x_n)v_n + \frac{h}{2}k(x, x_N)v_N \tag{9}$$

for $x \in [0, a]$. (Higher-order quadrature rules would not be appropriate if v is not known to be smooth.) Next define the matrix $\hat{K}$ and the column vectors $\hat{v}$ and $\hat{\mu}$ by

$$\hat{K} = (k_{mn})_{m,n=0}^N \qquad \hat{v} = (v_n)_{n=0}^N \qquad \hat{\mu} = (\mu_n)_{n=0}^N \tag{10}$$

where

$$k_{mn} = \begin{cases} k(x_m, x_n) & \text{for} \quad n \neq 0, N \\ \frac{1}{2}k(x_m, x_n) & \text{for} \quad n = 0, N \end{cases} \tag{11}$$

and $\mu_n = h^{-1}\mu(x_n)$, $v_n = v(x_n)$. The continuous problem (8) can then be written approximately as the minimization over all $\hat{v} \in R^{N+1}$ of

$$\min(\hat{K}\hat{v} - \hat{\mu})^\top(\hat{K}\hat{v} - \hat{\mu}) + \alpha h^2 \hat{v}^\top\hat{v} \tag{12}$$

with $\alpha = \tilde{\alpha}/h^4$. The discrete minimization problem is equivalent to the linear system

$$(\hat{K}^\top\hat{K} + \alpha h^2 I)\hat{v} = \hat{K}^\top\hat{\mu}. \tag{13}$$

The regularization parameter $\tilde{\alpha}$ plays an important role: it should be small enough that the minimization problem (8) approximates the original integral equation (4), and large enough that the discrete problem (12) is well posed. A well known principle for choosing a reasonable parameter α is based on the Morozov or damped Morozov discrepancy principle [14–19]. In the examples in this paper, we see that there is always a range of α, all below $\sim 10^{-4}$ (in most cases substantially below), which are adequate for stabilizing the calculation. The corresponding $\tilde{\alpha}$ are $\sim 10^{-11}$ or less, substantially below the scale $\|Kv\|^2/\|v\|^2 \sim 1$ at which the regularization would cause a significant change. Moreover, in all cases the recovered potential is essentially independent of the choice of α within these ranges.

2.3. Numerical experiments

Without loss of generality we take $a = 1$ throughout. Unless otherwise specified, we keep $M = 40$ terms in the sum over modes, and use $N = 40$ points in the discretization. (With $\sim M$ nodes in the interval, one needs $N \gtrsim M$ spatial points for adequate resolution.)

In the first series of examples (figure 1) we take the original potential to be $V(x) = 0$. The unperturbed spectrum $\{\lambda_n\}$ and the corresponding wavefunctions $\{f_n\}$ are trivially obtained analytically. We then subject this to different perturbations $\Delta V(x) = \epsilon U(x)$, where ϵ is a formal small parameter and for figure 1(a)–(c), U is respectively

$$U(x) = \sin(2\pi x) \tag{14}$$

$$U(x) = \begin{cases} 0, & x \in [0, 0.2) \\ 2x - \frac{2}{5}, & x \in [0.2, 0.7) \\ -\frac{10}{3}x + \frac{10}{3}, & x \in [0.7, 1] \end{cases} \tag{15}$$
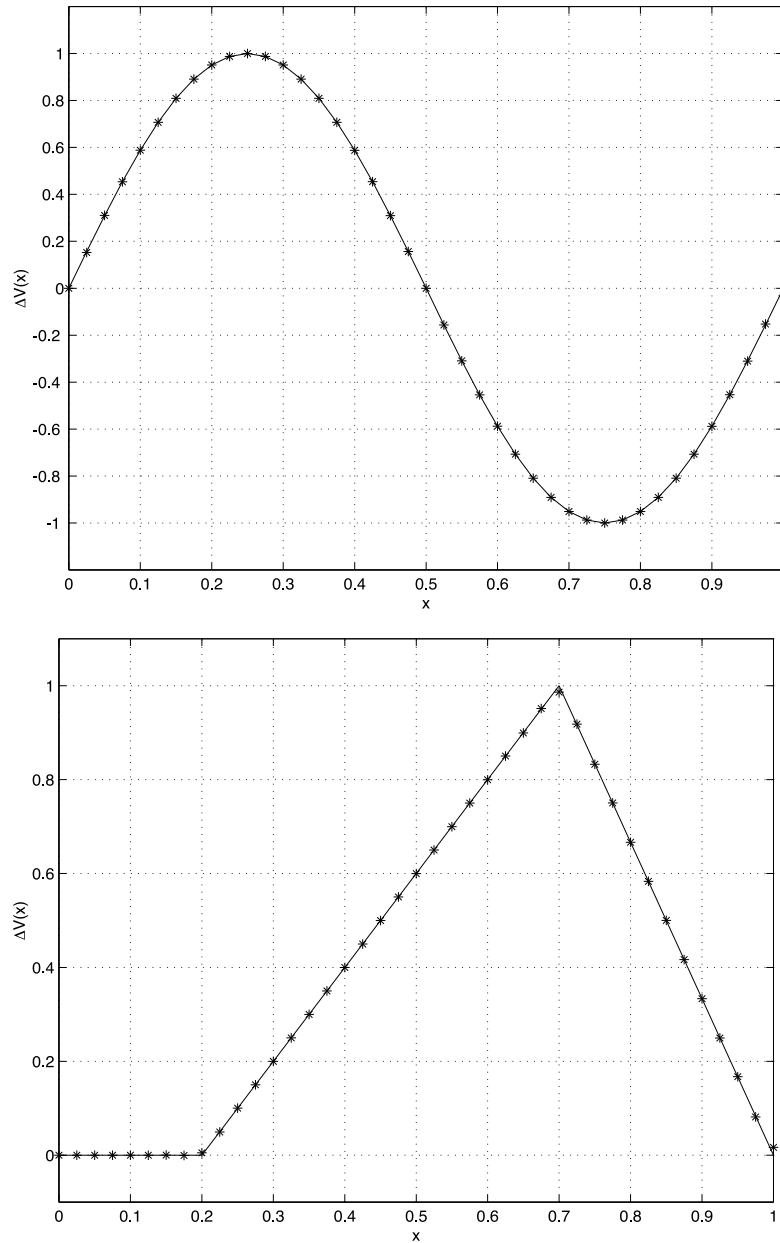
Figure 1. Perturbative inversion where the original potential is $V(x) = 0$ and the perturbation $\Delta V(x)$ is given by (14)–(16). The truncation is $N = M = 40$. The input ΔV is shown by the solid curve, and the reconstructed values are shown by the stars. The regularization parameter used was $\alpha = 10^{-8}$ in all three cases.

$$U(x) = \begin{cases} 2 - x, & x \in [0, 0.2) \\ 1 - x + 4x^2, & x \in [0.2, 0.7) \\ 3, & x \in [0.7, 1]. \end{cases} \qquad (16)$$

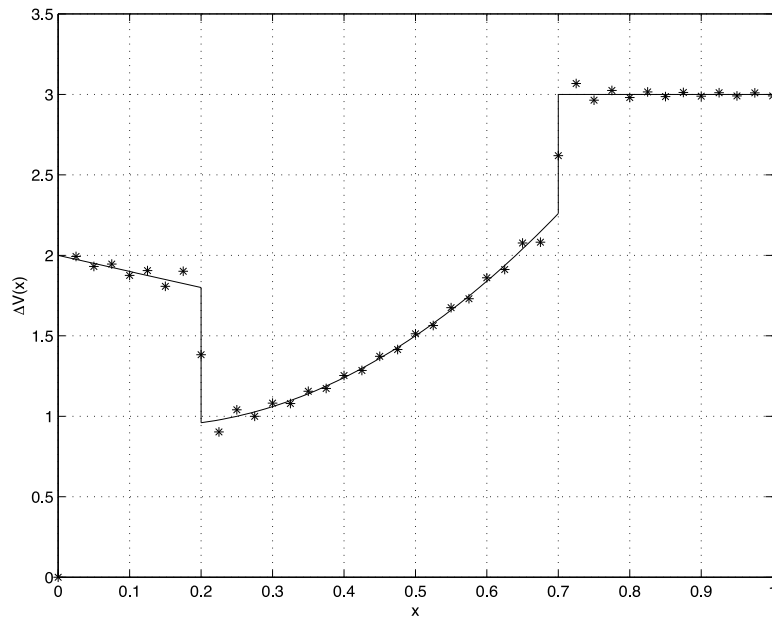The frequency shifts $\{\Delta\lambda_n\}$ are evaluated analytically by the forward formula (3) and then

Figure 1. (Continued)

used in the inversion scheme described above. The regularization parameters used in the three examples are all $\alpha = 10^{-8}$. Essentially the same results are obtained for a large range of α; as an example, for figure 1(a), the L^2 relative error is not more than $\sim 5 \times 10^{-3}$ for all $\alpha \in [10^{-12}, 10^{-6}]$.

For smooth perturbations, one could use a much coarser grid of discretization, and correspondingly truncate the sum to fewer modes. Figure 2(a) shows the perturbing potential (14) recovered with $N = M = 6$, again with $\alpha = 10^{-8}$. The recovery is nearly perfect, except for the endpoint $x = a$. This problem is readily understood if the potential is viewed in terms of the extended interval $[0, 2a]$: there is a cusp at $x = a$ and the potential is in fact not smooth. Figure 2(b) shows the analogous recovery for the potential $U(x) = \sin(3\pi x/2)$; this does not have a cusp, and the recovery does not run into any problem at the endpoints even with a coarse grid.

To see the effect of the parameters $\{\sigma_n\}$, we have tried one example with ΔV being a step (figure 3), and $\sigma_n = n^{3/2}$ (figure 3(a)); $\sigma_n = n^2$ (figure 3(b)); $\sigma_n = n^3$ (figure 3(c)). These show that a range of choices including $\sigma_n = n^2$ all give acceptable results. Discontinuous potentials are more susceptible to noise, and a slightly larger α is needed ($\sim 10^{-5}$).

In the next series of examples (figure 4) we take the original potential to be $V(x) = (x - 2a)^2$, to illustrate that the algorithm works just as effectively when $V \neq 0$. The unperturbed eigenvalues and eigenfunctions have to be first evaluated numerically, using the standard piecewise linear finite-element method to reduce the eigenvalue equation to a system of linear algebraic equations [20]. In this forward step, in order to get M modes accurately, many more spatial points $N' \gg M$ need to be used. In this case, $M = 40$ and one can choose $N' = 80$ or 120. The perturbations used are exactly those in (14)–(16). It is clear from these examples that the method works satisfactorily.
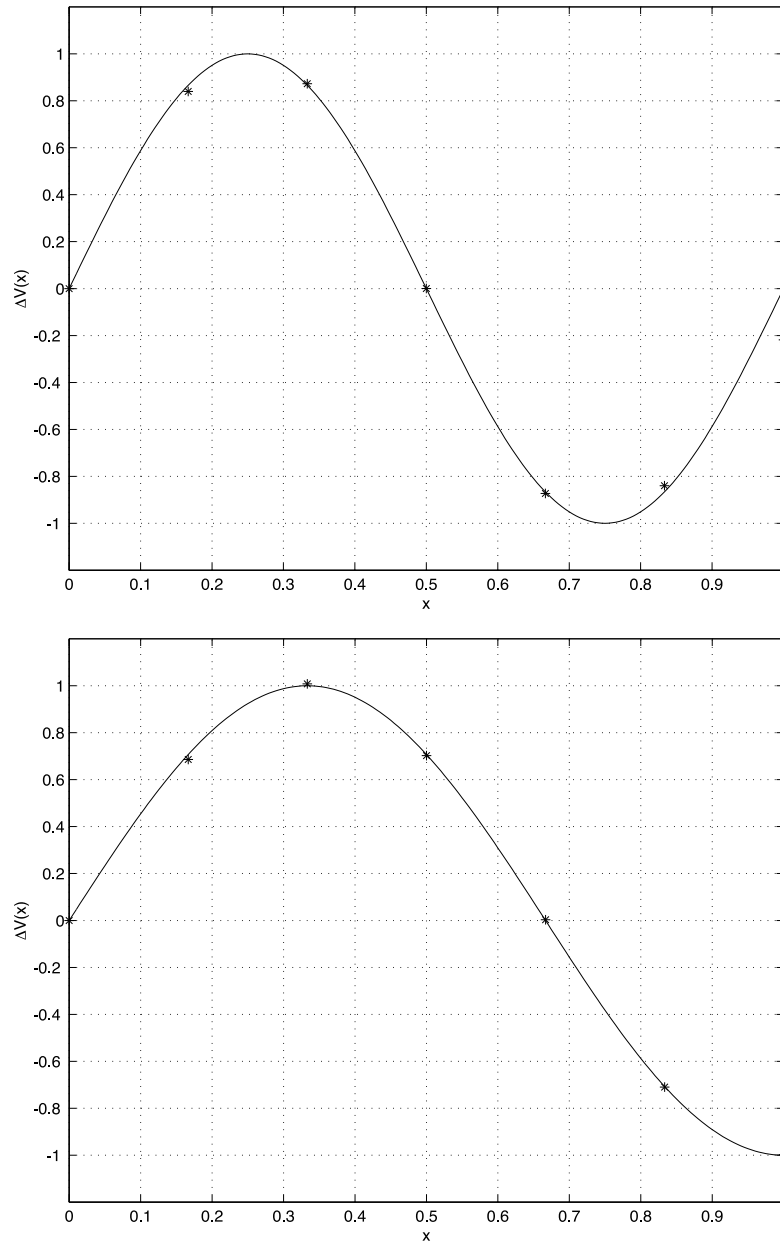
Figure 2. (*a*) Perturbative inversion of a smooth potential (same as figure 1(*a*)) using $N = M = 6$. The forward problem is evaluated analytically and exactly. The regularization parameter used was $\alpha = 10^{-8}$. (*b*) Similar perturbative inversion for a potential without a cusp on the extended interval.

3. Total inversion

In this section we show how TI can be achieved by an iterative process of PI. To describe the method, and to exhibit its formal similarity with Newton's method for the solution of equations, it will be useful to adopt an abstract notation. Let all the eigenvalues and eigenfunctions be
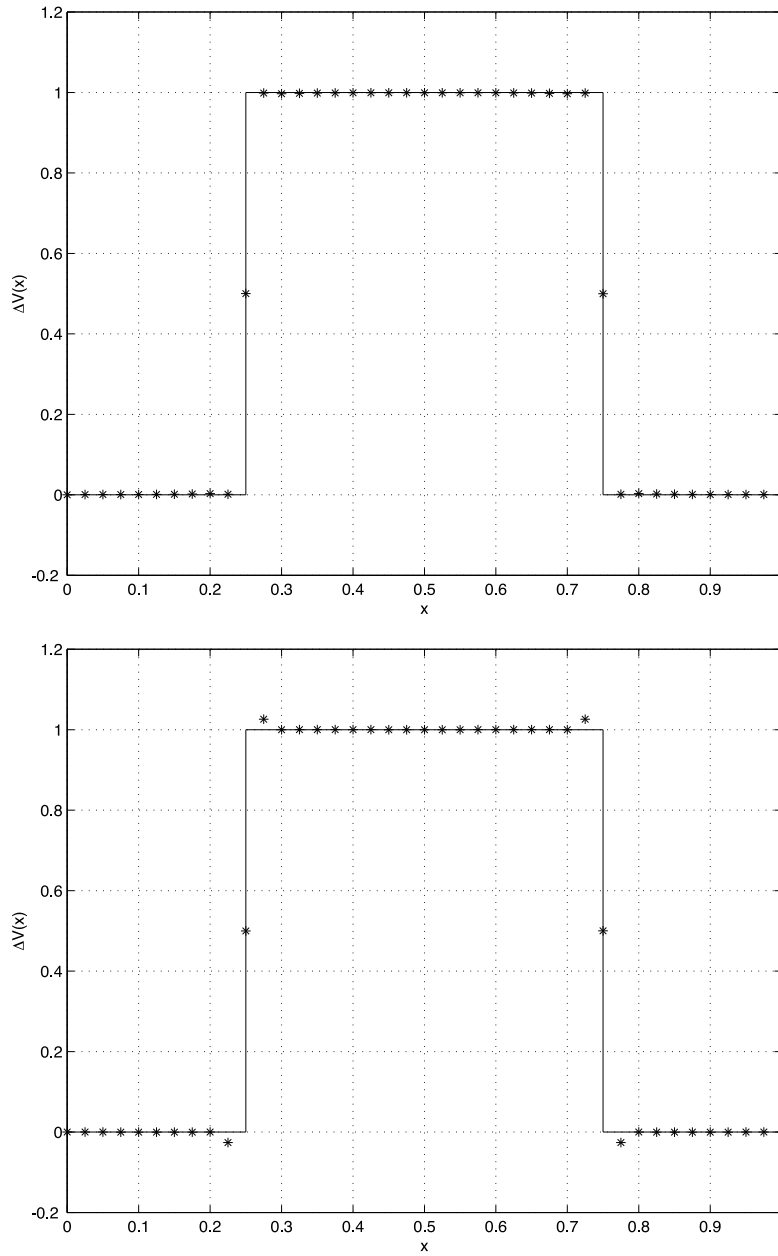
Figure 3. Perturbative inversion where the original potential is $V(x) = 0$ and the perturbation $\Delta V(x)$ is a step, using (*a*) $\sigma_n = n^{3/2}$, (*b*) $\sigma_n = n^2$, (*c*) $\sigma_n = n^3$ and in all cases $N = M = 40$. The input ΔV is shown by the solid line, and the reconstructed values are shown by the stars. The regularization parameter used was $\alpha = 10^{-5}$ in all cases.

collectively denoted as $\lambda \equiv \{\lambda_n\}$ and $f \equiv \{f_n\}$, and let the potential be simply denoted as V. The eigenvalues are determined by the potential, which we express as a functional relation:
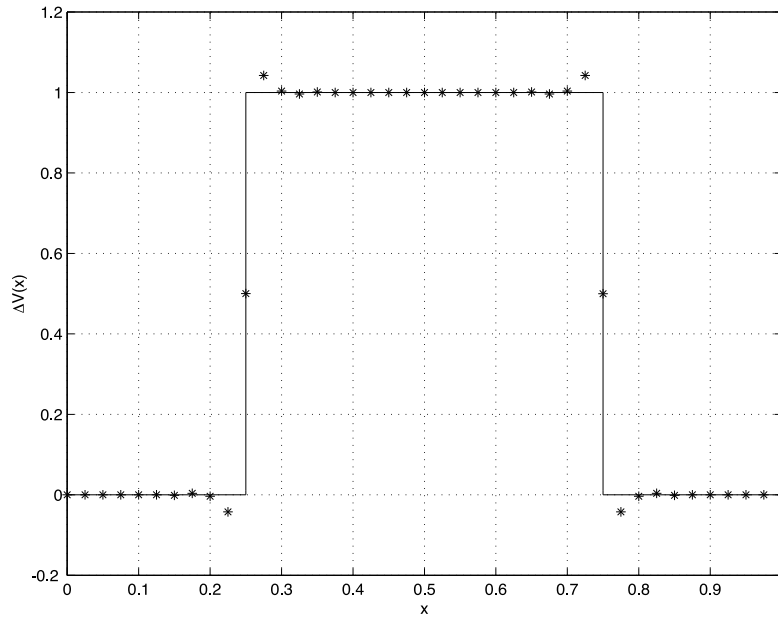
$$\lambda = \mathcal{F}(V). \tag{17}$$

Figure 3. (Continued)

The forward perturbative expression (3) is then written schematically as a functional derivative

$$\Delta\lambda = \frac{\delta\mathcal{F}}{\delta V}\Delta V \tag{18}$$

while the PI methodology described in sections 2.2 and 2.3 provides the action of the inverse functional derivative

$$\Delta V = \left[\frac{\delta\mathcal{F}}{\delta V}\right]^{-1}\Delta\lambda \tag{19}$$

for any given $\Delta\lambda$ and any unperturbed potential V.

Now the problem of TI is to find a potential V that satisfies (17), when λ is prescribed. The process is now obvious. Start with an initial guess $V(0)$ (which we shall simply take to be the zero potential), and construct a series of improvements $V(j)$ as follows. (a) For any $V(j)$, calculate the eigenvalues $\lambda(j) = \mathcal{F}(V(j))$ and the corresponding eigenfunctions $f(j)$. (b) The next iteration is then obtained by Newton's algorithm:

$$V(j+1) = V(j) - \left[\frac{\delta\mathcal{F}}{\delta V}\right]^{-1}[\lambda(j) - \lambda] \tag{20}$$

where $[\delta\mathcal{F}/\delta V]^{-1}[\lambda(j) - \lambda]$ is obtained by PI, in which K and μ are calculated using the eigenfunctions $f(j)$ found in the last step.

There are two measures of convergence:

$$\begin{aligned} D_{j+1}^2 &= \|V(j+1) - V(j)\|^2 \\ \Delta_j^2 &= \|\lambda(j) - \lambda\|^2 \equiv \sum_n |\lambda_n(j) - \lambda_n|^2 \end{aligned} \tag{21}$$

where in practice n is summed over the M modes under consideration. The iteration is stopped when D_{j+1} is less than a preset tolerance.
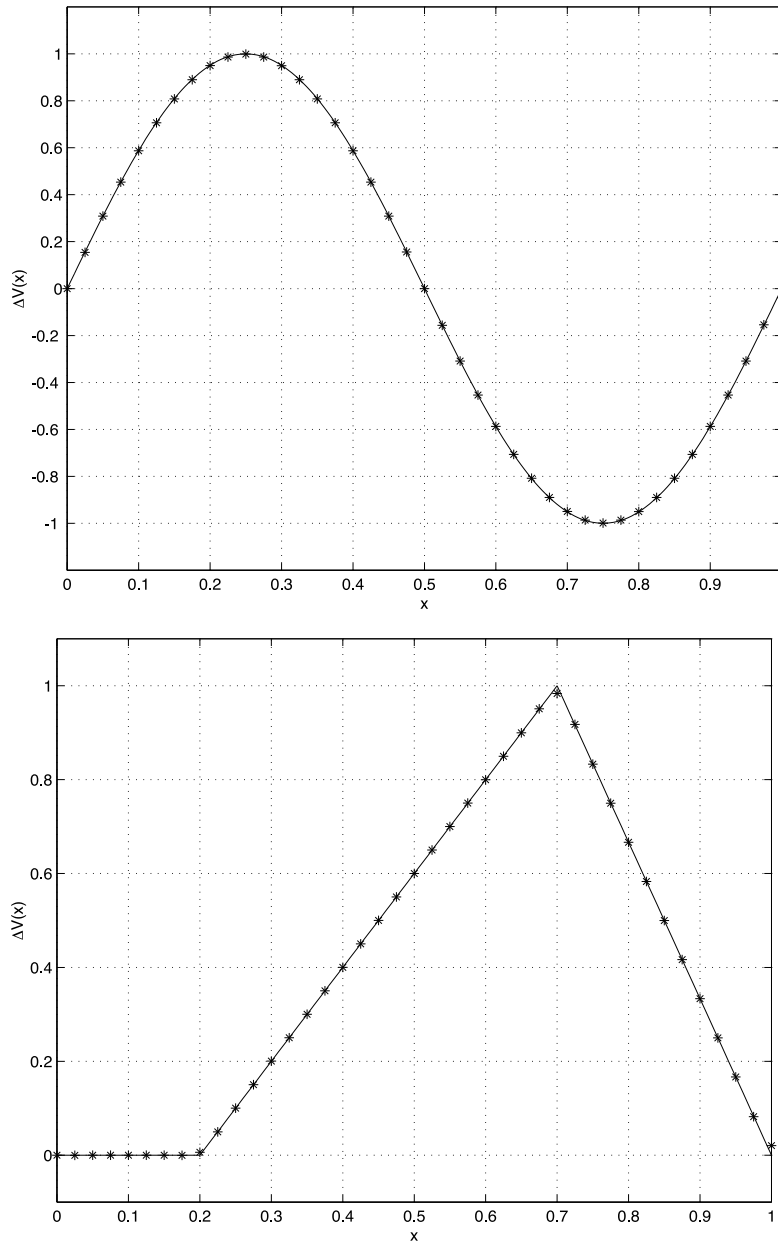
Figure 4. Perturbative inversion where the original potential is $V(x) = (x - 2a)^2$ and the perturbation $\Delta V(x)$ is given by (14)–(16). The truncation was $N = M = 40$. The input ΔV is shown by the solid curve, and the reconstructed values are shown by the stars. The regularization parameter used was $\alpha = 10^{-8}$ in all cases.

Figure 5 shows the implementation of this algorithm, using $V(x) = U(x)$ (without a formal small parameter ϵ), where U are the three potentials in (14)–(16). The starting potential is zero, and each figure shows the potential reconstructed after one and two iterations (except for figure 5(*b*), where the potentials recovered after the first and second iterations are too close
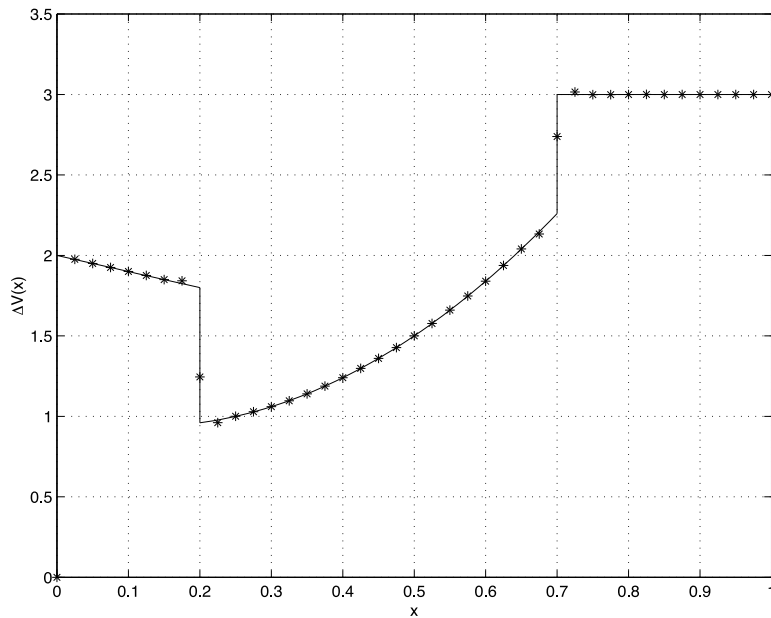
Figure 4. (Continued)

to distinguish). In all cases, the tolerance of 10^{-2} was reached in only two iterations.

For smooth potentials such as that in figure 5(a), it is again possible to achieve accurate total inversion using very few points and very few iterations (figure 6(a)). Also, to illustrate the situation when the potential is large (so that $V = 0$ would be a poor initial guess), figures 6(b) (c) show the result of TI for the same potential scaled up by factors of 10 and 50, respectively. Since the starting point ($V = 0$) is farther from the solution, more iterations are required, as expected. In these examples using a coarse mesh, there is again a small problem at one endpoint; as with figure 2, this problem would not occur if the potential does not have a cusp on the extended interval.

Further convergence beyond two steps is difficult to show in figure 5; instead, it is more convenient to see how the two measures of convergence depend on j. Figure 7 plots $\ln |\ln D_j|$ versus j for the examples of figure 5; those for $\ln |\ln \Delta_j|$ are similar and not shown. These plots agree asymptotically with the form $j \ln 2 + \text{const}$ expected from Newton's method, indicating the very rapid rate of convergence.

4. Conclusion

In this paper we have constructed an efficient algorithm for the inversion of the potential of a conservative system from its NM spectra, based on numerical techniques that are well established and familiar. The trick is to first consider the linear problem of PI, and then to reduce the more difficult problem of TI, through a Newton-like method, to a series of linear steps as well. The method has been shown to be stable and accurate, and convergence in the TI case is rapid. The method is therefore a practical one when the spectra are known.

The size of the truncation required (N or M) depends on two factors. First, if the spatial resolution required (say the typical length scale of variation of V) is δ, then one obviously needs $M > M_\delta = a/\delta$. There is, however, another condition. Let the range of the potential
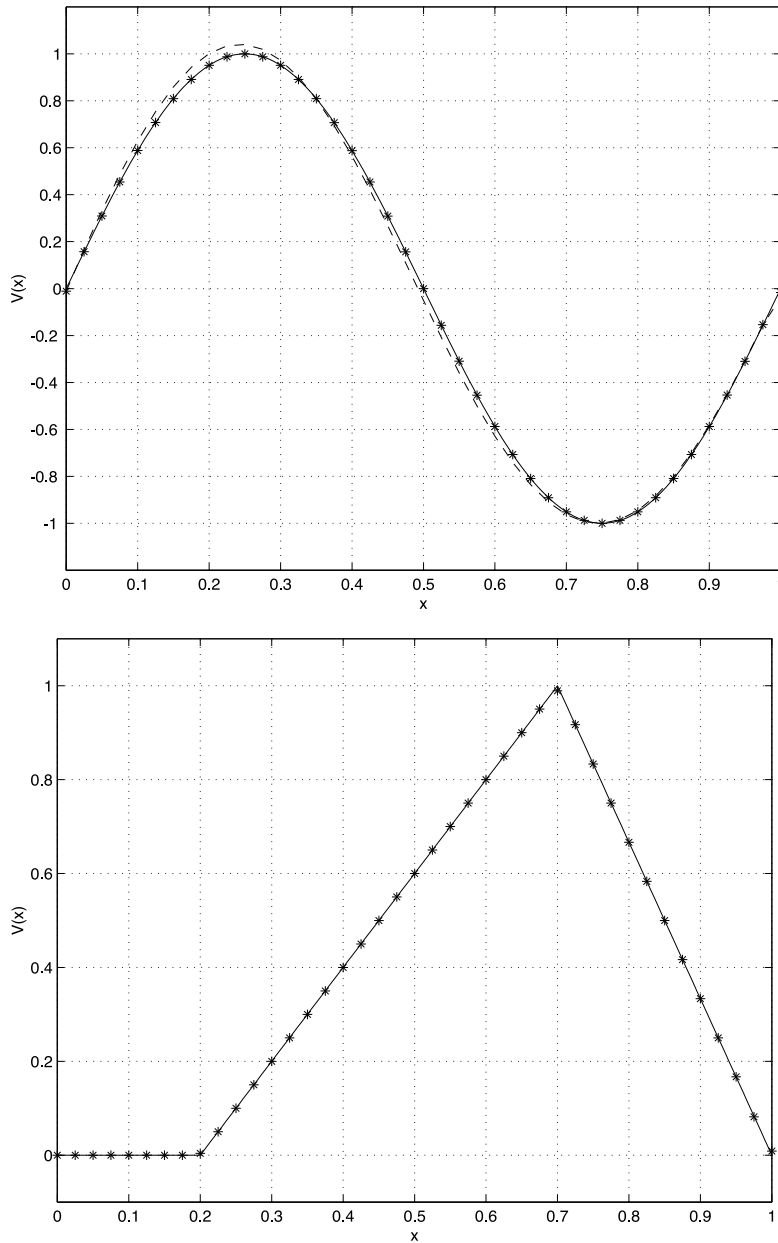
Figure 5. Total inversion of potential $V(x) = U(x)$ and $U(x)$ is given by (14)–(16). The input V is shown by the solid curve. In (*a*) and (*c*), the first iterate is shown by the broken curve, and the second iterate by the stars. In (*b*), the first iterate is too close to the second, and is not shown. The regularization parameter used was $\alpha = 10^{-4}$ in all cases.

and hence the range of the kinetic energy be $R = \max(V) - \min(V)$. Identifying the kinetic energy for each mode n approximately with $(n\pi/a)^2$, we see that the number of modes that must be retained should satisfy $M > M_R \equiv (a/\pi)\sqrt{R}$. Applied to the case in figure 6(*c*) with $a = 1$, $R = 50$, we find $M_R \approx 1$, so truncation to $M = 6$ is adequate.
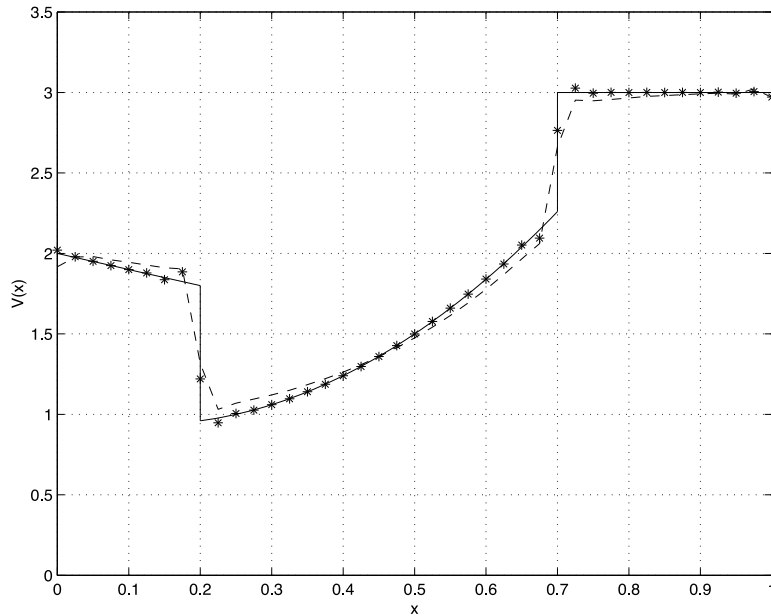
Figure 5. (Continued)

An intriguing question is whether the method can be generalized to *open, nonconservative* systems, e.g., the same differential equation (1) on $I = [0, a]$, with a real potential $V(x)$ (no absorption) but with outgoing boundary conditions at one end. One can think of I as an optical cavity, with a partially transmitting mirror at $x = a$; in fact the scalar model of electromagnetism in such a cavity [21] is described by a wave equation to which this KG equation can be transformed [22].

In such open systems, the analogue to the NMs are quasinormal modes (QNMs), which are factorized solutions $\Phi(x, t) = f(x)e^{-i\omega t}$ with $\mathrm{Im}\,\omega < 0$ because energy or probability are carried off by the outgoing waves. Thus, open systems are physically nonconservative and mathematically not self-adjoint, so that the equations are no longer of a Sturm–Liouville type. Nevertheless, in a broad class of such systems the QNMs are complete [23,24], and a formalism can be developed that closely parallels that for NMs in closed, conservative systems [22,25,26].

It is thus natural to attempt a generalization of the NM inversion formalism to QNMs. For NMs on $[0, a]$, *two* sets of eigenvalues are required: the nodal and antinodal set as described in section 1. However, each QNM eigenvalue ω is *complex*, and in a sense carries twice the amount of information. Thus, one might conjecture that *one* set of eigenvalues, corresponding to *one* boundary condition (i.e., outgoing waves at $x = a$) would be sufficient. A generalization of the present formalism to nonconservative systems would help to answer this conjecture.

A potential application concerns gravitational waves emitted by matter falling into black holes. These waves, in each angular momentum sector, are described by a KG equation [27]. Numerical experiments [28] show that the signal could be dominated by QNMs [29] in many cases. Their complex frequencies can be extracted from the signal, but would not be those of a bare black hole; instead, they are those of a black hole perturbed by its astrophysical environment—a *dirty* black hole [30]. If the perturbation, i.e., the astrophysical environment, can be ascertained from the frequency shifts through a PI algorithm, then one could begin to develop a new tool for gravitational wave astronomy. Thus the inversion problem for open
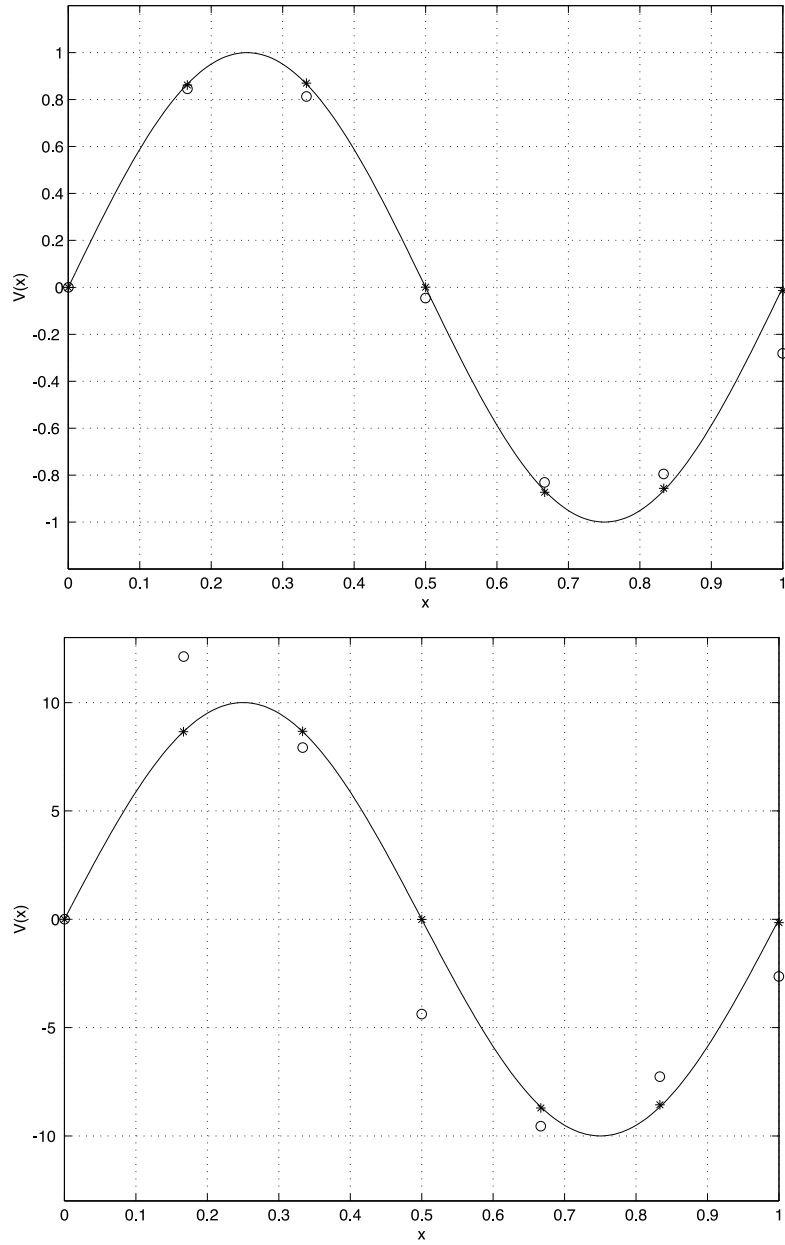
Figure 6. (*a*) Total inversion of the smooth potential in figure 5(*a*), using $N = M = 6$. The circles are the first iterate and the stars the second iterate. (*b*) Total inversion for 10 times the potential. The circles shows the first iterate and the stars show the fourth iterate. (*c*) Total inversion for 50 times the potential. The circles show the second iterate and the stars show the sixth iterate. The regularization parameter used was $\alpha = 10^{-4}$ in all cases.
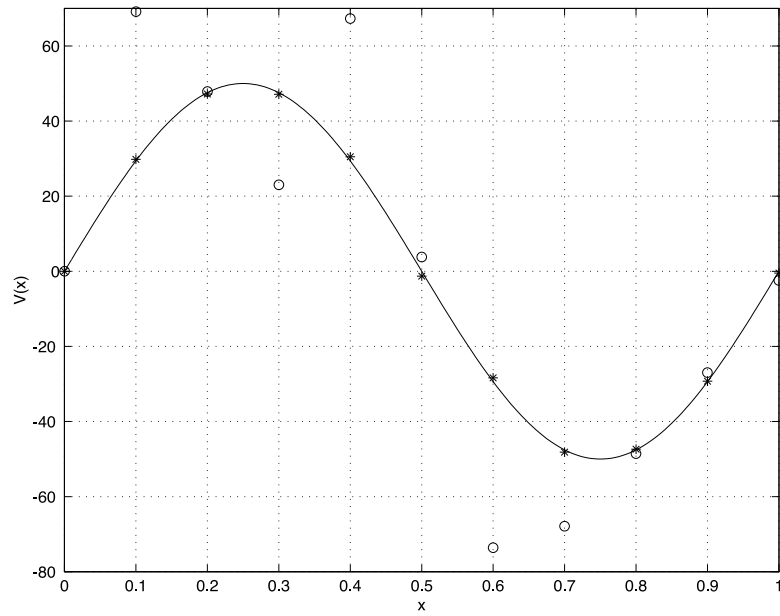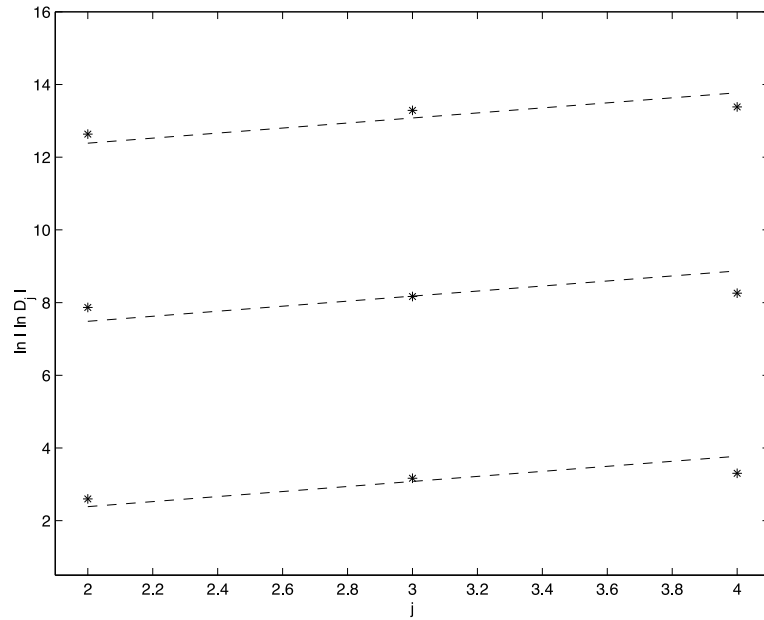
Figure 6. (Continued)

Figure 7. A plot of $\ln | \ln D_j |$ versus j corresponding to the three examples in figure 5 (from top to bottom). The stars in each series have been displaced vertically for clarity. The lines are drawn with slope $\ln 2$, which is the behaviour expected from Newton's method.

systems is of great interest, since gravitational waves are likely to be detected in the next decade [31]. Work on nonconservative systems will be reported elsewhere.

Acknowledgments

This work is supported in part by the Hong Kong Research Grants Council: that of KY by grant no 4006/98P and that of JZ by grant no 4004/98P. CPS has been supported by a C N Yang Visiting Fellowship. The authors thank Y T Chan for carrying out the numerical experiments. We have benefited from discussions with W S Lee, P T Leung, S H Ling, A Maassen van den Brink, W-M Suen, S Wong and C M Yip. In particular we thank A Maassen van den Brink for pointing out the reason for the problem at the endpoint in figures 2(*a*) and 6.

References

[1] Bargmann V 1949 *Phys. Rev.* **75** 301
    Bargmann V 1949 *Rev. Mod. Phys.* **21** 488
[2] Borg G 1946 *Acta Math.* **78** 1
[3] Levinson N 1949 *Math. Tidsskr.* B **25** 24
[4] Marchenko V A 1950 *Dokl. Akad. Nauk* SSSR **72** 457
    Marchenko V A 1955 *Dokl. Akad. Nauk* SSSR **104** 695
[5] Krein M G 1951 *Dokl. Akad. Nauk* SSSR **76** 21
    Krein M G 1951 *Dokl. Akad. Nauk* SSSR **76** 345
    Krein M G 1952 *Dokl. Akad. Nauk* SSSR **82** 669
[6] Jost R and Kohn W 1952 *Phys. Rev.* **87** 979
    Jost R and Kohn W 1952 *Phys. Rev.* **88** 382
[7] Gelfand I M and Levitan B M 1951 *Izv. Akad. Nauk.* SSSR, Ser. Mat. **15** 309 (Engl. Transl. 1955 *Am. Math. Soc. Trans.* **1** 253)
    Levitan B M 1964 *Izv. Akad. Nauk* SSSR Ser. Mat. **28** 63
    Levitan B M and Gasymov M G 1964 *UMN* **19** 3 (Engl. Transl. 1964 *Russ. Math. Sur.* **19** 1)
[8] Faddeev L D 1959 *Usp. Mat. Nauk* **14** 57 (Engl. Transl. Seckler B 1963 *J. Math. Phys.* **4** 72)
[9] Dyson F J 1976 *Essays in Honor of Valentine Bargmann* ed E H Lieb, B Simon and A S Wightman (Princeton, NJ: Princeton University Press)
[10] Levitan B M 1987 *Inverse Sturm Liouville Problems* (Utrecht: VNU Science)
[11] Barcilon V 1986 *Inverse Eigenvalue Problems (Lecture Notes in Mathematics vol 1225)* ed A Dold and B Eckmann (Berlin: Springer) p 1
[12] Lowe B D, Pilant M and Rundell W 1992 *SIAM J. Math. Anal.* **23** 482
    Kirsch A 1996 *An Introduction to the Mathematical Theory of Inverse Problems* (New York: Springer)
[13] Zakhariev B N and Suzko A A 1990 *Direct and Inverse Problems, Potentials in Quantum Scattering* (New York: Springer)
    Gladwell G M L 1993 *Inverse Problems in Scattering, an Introduction* (Dordrecht: Kluwer)
[14] Groetsch C W 1983 *The Theory of Tikhonov Regularization for Fredholm Equations of the First Kind* (Boston, MA: Pitman)
[15] Kunisch K and Zou J 1998 *Inverse Problems* **14** 1247
[16] Ito K and Kunisch K 1992 *SIAM J. Optim.* **2** 376
[17] Kunisch K 1993 *Computing* **50** 185
[18] Louis A K 1989 *Inverse und Schlechtgestellte Problems* (Stuttgart: Teubner)
[19] Morozov V A 1984 *Methods for Solving Incorrectly Posed Problems* (New York: Springer)
[20] Strang G and Fix G 1988 *An Analysis of the Finite Element Method* (Wellesley: Wellesley-Cambridge)
[21] Lang R, Scully M O and Lamb W E 1973 *Phys. Rev.* A **7** 1788
[22] Leung P T, Tong S S and Young K 1997 *J. Phys. A: Math. Gen.* **30** 2139
    Leung P T, Tong S S and Young K 1997 *J. Phys. A: Math. Gen.* **30** 2153
[23] Leung P T, Liu S Y and Young K 1994 *Phys. Rev.* A **49** 3057
    Leung P T, Liu S Y, Tong S S and Young K 1994 *Phys. Rev.* A **49** 3068
    Leung P T, Liu S Y and Young K 1994 *Phys. Rev.* A **49** 3982
[24] Ching E S C, Leung P T, Suen W M and Young K 1995 *Phys. Rev. Lett.* **74** 4588
    Ching E S C, Leung P T, Suen W M and Young K 1996 *Phys. Rev.* D **54** 3778
[25] Leung P T, Suen W M, Sun C P and Young K 1998 *Phys. Rev.* E **57** 6101
[26] Ching E S C, Leung P T, Maassen van den Brink A, Tong S S, Suen W M and Young K 1998 *Rev. Mod. Phys.* **70** 1545

[27] Chandresekhar S 1991 *The Mathematical Theory of Black Holes* (Chicago, IL: Chicago University Press)
[28] Anninos P, Hobill D, Seidel E,Smarr L and Suen W M 1993 *Phys. Rev. Lett.* **71** 2851
Anninos P, Hobill D, Seidel E,Smarr L and Suen W M 1995 *Phys. Rev.* D **52** 2044 and references therein
[29] Leaver E W 1985 *Proc. R. Soc.* A **402** 285
Leaver E W 1992 *Class. Quantum Grav.* **9** 1643
[30] Leung P T, Liu Y T, Suen W M, Tam C Y and Young K 1997 *Phys. Rev. Lett.* **78** 2894
Leung P T, Liu Y T, Suen W M, Tam C Y and Young K 1999 *Phys. Rev.* D **59** 044034
[31] Abramovici A A *et al* 1992 *Science* **256** 325